

Crop water stress mapping for site-specific irrigation by thermal imagery and artificial reference surfaces

M. Meron · J. Tsipris · Valerie Orlov · V. Alchanatis ·
Yafit Cohen

Published online: 26 January 2010
© Springer Science+Business Media, LLC 2010

Abstract Variable-rate irrigation by machines or solid set systems has become technically feasible, however mapping crop water status is necessary to match irrigation quantities to site-specific crop water demands. Remote thermal sensing can provide such maps in sufficient detail and in a timely way. In a set of aerial and ground scans at the Hula Valley, Israel, digital crop water stress maps were generated using geo-referenced high-resolution thermal imagery and artificial reference surfaces. Canopy-related pixels were separated from those of the soil by upper and lower thresholds related to air temperature, and canopy temperatures were calculated from the coldest 33% of the pixel histogram. Artificial surfaces that had been wetted provided reference temperatures for the crop water stress index (CWSI) normalized to ambient conditions. Leaf water potentials of cotton were related linearly to CWSI values with $R^2 = 0.816$. Maps of crop stress level generated from aerial scans of cotton, process tomatoes and peanut fields corresponded well with both ground-based observations by the farm operators and irrigation history. Numeric quantification of stress levels was provided to support decisions to divide fields into sections for spatially variable irrigation scheduling.

Keywords Cotton · Peanut · Process tomato · Crop water stress index (CWSI) · Leaf water potential · Thermography

Introduction

Site-specific irrigation may be defined as matching water application in time and quantity to actual crop needs at the smallest manageable scale to achieve the desired crop responses. As variable-rate water application technology is already available, field scale application

M. Meron (✉) · J. Tsipris · V. Orlov
Crop Ecology Laboratory, MIGAL Galilee Technology Center, PO Box 831, Kiryat Shmona, Israel
e-mail: meron@migal.org.il

V. Alchanatis · Y. Cohen
Institute of Agricultural and Environmental Engineering, Agricultural Research Organization,
Volcani Center, Bet Dagan, Israel

will depend on the ability to map the variation in crop water status (Camp et al. 2006). Devices for point sensing of soil or crop water status that use wireless communication are abundant and can be connected to the irrigation machines for real time control (e.g. Peters and Evett 2004; Kim et al. 2007). Applying enough of them to match the spatial variability, however will be prohibitive in terms of cost with current technology (Or 1995; Schmitz and Kuyper 1998; Schmitz and Sourell 2000). Remote thermal imagery is a viable alternative to point measurements, since the canopy temperature of the whole field can be measured at once, and a map of the distribution of plant water status in the field can be produced.

Evaluation of relevant crop temperatures by pattern recognition of sunlit leaves (Leinonen and Jones 2004; Cohen et al. 2005) may approximate the theoretical ‘big leaf’ temperature for heat balance calculations. However, this method is limited to very fine pixel resolutions and it requires exact co-registration of the thermal image with the visible one, which limits the practicality of aerial surveys. Histogram processing of image frames, taken at a pixel size of less than half the width of the cropped fraction in a partially covered canopy, enables separation of canopy from soil temperatures as they correspond to different portions of the histogram (Meron 1987). The coldest 33% of the remaining canopy related pixels after separating soil can be used as the representative ‘cold’ crop temperature for water stress evaluation, as demonstrated in Meron and Charitt (2003). More detailed evidence to support this procedure is in preparation.

The widely accepted concept of the crop water stress index (CWSI) (Jackson et al. 1981) is defined as a fraction of the canopy temperature between an upper (dry) and a lower (wet) reference under ambient conditions. The relation between ambient conditions and a variety of baselines and references have been investigated over the years. Empirical well watered base lines introduced initially with CWSI were found later to be strongly related to specific conditions (Idso 1982). Temperatures of natural surfaces such as a well watered crop (Gardner et al. 1992a, b) are good indicators, but such surfaces need dedicated maintenance, which impedes the implementation of this approach at the production scale. Reference temperatures derived from foliage that has been wetted or greased are mainly useful for micro-scale methods (Jones, 1999). Wetted reference surfaces constructed of manmade materials are well-defined and reproducible indicators of ambient conditions, with some limitations at non-turbulent wind velocities (Meron and Charitt 2003).

The area covered by a thermal survey system is defined by swath width (sensor array width multiplied with the pixel size on the ground) and velocity. Pixel size is limited to the largest size that will enable the separation of soil temperatures and detection of fractions of canopy temperature; this is usually smaller than half of the width covered by the crop row. Flight velocity is limited by shutter speed, which determines pixel sharpness. Cooled imagers are fast and sharp, but expensive. Bolometric thermal imagers are more widely used because they are more affordable. However, their acquisition speeds of 1/140 to 1/200 s are too slow to freeze motion. Aerial or ground surveys with bolometric cameras must slow down to eliminate blur, or the processing must be able to handle blurred images and enlargement of the pixel size because of pixel ‘smear’ in the direction of movement.

Economic thermal mapping depends on the system’s capacity to cover the area in a given time. One of the options to enhance the capacity is to skip swaths and frames, and then interpolate CWSI values to generate maps.

The objective of this work was to establish the relation of crop stress properties to a remotely measured thermal index, and to explore the feasibility of mapping crop stress by remote thermography for site-specific irrigation.

Materials and methods

High resolution ground surveys on a single field

Location

Ground-based measurements were obtained during the summer of 2007 at a commercial cotton (*Gossypium hirsutum* x *barbadense* hybrid c.v. Acalpi) field in the Hula Valley of Israel (N33.11, E35.35). The soil at the site is a brown alluvial hydromorphic gromosol, and the climate is Mediterranean. The field was selected as an experimental site from previous observations of variable crop development, apparently related to very variable soil water-holding characteristics caused by the spatially variable alluvial deposits. The cotton was planted in 0.96 m spaced rows, cultivated by conventional methods, and was free of pests and diseases. The crop was irrigated uniformly with a lateral moving sprinkler system. Irrigation was scheduled by the grower, based on recommendations from the extension service and available water supply. Potential evapo-transpiration (ET_p) was evaluated from a nearby weather station by a modified Penman formula, similar to the CIMIS grass reference (Craddock 1994) method. Watering dates and amounts related to ET_p are shown in Fig. 1.

Thermography

A FLIR (Billerica, MA) model SC2000 radiometric infrared (IR) camera, equipped with a 45° FOV lens, was mounted about 5 m above crop level, 3 m left of the boom center and pointing straight down 180° to zenith on the spraying boom of a TECNOMA model “Laser 4000” self propelled, high pass sprayer (Epernay, France) (Fig. 2). The camera was remotely controlled by FLIR ThermoCam™ software on an IBM ThinkPad laptop. A GPS receiver (MID-TECH model RX 400p) with 1–3 m spatial accuracy was mounted on the

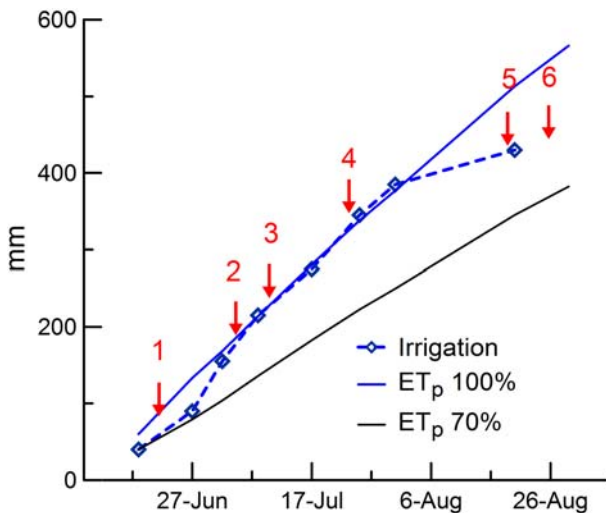


Fig. 1 Evaporative demand (70 and 100% ET_p), irrigation amounts and survey events (arrows) in the monitored field at the Hula Valley 2007



Fig. 2 Infrared scanner mounted on a high pass sprayer

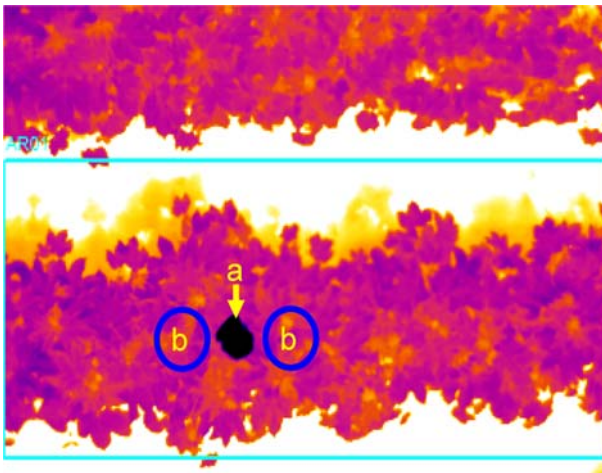


Fig. 3 False color IR image of a cotton row: **a** location marker and plant height measuring stick and **b** leaf water potential (LWP) sampling points

sprayer and connected to the same computer. Images were captured and locations were measured every second. The IR images were matched to location by the computer's clock.

Sampling

Ten sampling sites were selected along a crop row that displayed very variable soil water holding capacity and were marked with a 2 m high fiberglass pole for repeated examinations (Fig. 3). The sites were selected by a visual examination of crop development before

the start of irrigation. Two young, sunlit, fully expanded leaves within 0.5 m of each marking pole were sampled for leaf water potential (LWP) using a pressure chamber (Ari-Mad, Israel). The LWP was determined on every scanning day within 15 min of the field scan. Leaves to be used for LWP analysis were wrapped with aluminum foil at cutting and pressurized while wrapped as described by Meron et al. (1987). Plant height from ground level to the main stem tip was recorded weekly on the marking pole for each sampled plant until the cessation of growth.

Meteorology and reference surfaces

The artificial reference surface (ARS) was placed at the edge of the field, together with the weather station. It consisted of a wet, white, non-woven viscose-polyester fabric in a double layer covering a polystyrene float. The float was placed in a 0.4×0.3 m water-filled plastic box, and the fabric was kept constantly wet via a wick from the water. An Apogee (Logan UT) IR thermal sensor mounted 0.1 m above the surface recorded ARS temperatures. The sensor was connected to a Campbell Scientific (Logan UT) system comprising a CR10X data logger, an air temperature and relative humidity sensor (Vaisala model HMP50), a global radiation sensor (Li-Cor model 200X) and a rotating cup anemometer (RM Young model 3101) at 2 m elevation. Values were measured at intervals of 6 s and averages were recorded every minute.

Image processing

Images were processed in Visual Basic 5 using OLE automation functions provided in the FLIR Researcher™ package. First, the histogram of the image was constructed with 256 bins in the 19–45.5°C range and an interval of 0.1°C. Next, only pixels within the temperature limit described by Eq. 1 were retained, assuming that temperatures outside this range are not canopy-related.

$$(T_{\text{air}} - 10) < T_{\text{pixel}} < (T_{\text{air}} + 7), \quad (1)$$

where T_{air} (°C) is air temperature and T_{pixel} (°C) is the calibrated pixel temperature. The cumulative average weights of the coldest 33% pixels were calculated by Eq. 2.

$$T_{\text{canopy}} = \frac{\sum_{i=1}^{0.33N} T_i * f_i}{\sum_{i=1}^{0.33N} f_i}, \quad (2)$$

where T_i (°C) is the temperature, f_i is the number of pixels in each i th class of the histogram and $0.33N$ is 33% of the pixels retained at the first step after the non crop related pixels were discarded. The CWSI was subsequently calculated by Eq. 3:

$$CWSI = \frac{T_{\text{canopy}} - T_{\text{ARS}}}{T_{\text{air}} + 5^\circ - T_{\text{ARS}}}, \quad (3)$$

where T_{canopy} is the mean temperature of the 33% coldest pixels after discarding pixels hotter than 7°C from the air, T_{ARS} is the wet ARS temperature and T_{air} is air temperature (°C) at the time of image acquisition.

Crop cover was determined by dividing the number of plant related pixels by the total number of pixels per square meter in the frame.

Survey and mapping

Six ground surveys were performed throughout the season. Swath widths were 4.5 m, except for the first survey which had 1.5 m swath widths. Frames were recorded every 3 m along the row, and the resulting frame area covered was 4.5–13.5 m² corresponding to the swath width. Distance between swaths ranged from 12 to 24 m. Survey dates and the relevant details are given in Table 1.

The center point of each CWSI frame was assigned to the corresponding GPS location as a point feature in an ArcView 9.2 GIS map (ESRI, Redland CA). The resulting grid densities of the CWSI points ranged from 3 × 24 m to 3 × 12 m (Table 1). Maps were generated by inverse distance weighted (IDW) interpolation of the CWSI points using inbuilt functions of ArcView 9.2 Spatial Analyst extension.

Aerial survey

To test the feasibility of the proposed method at a larger scale, an aerial survey was conducted over several field crops in the Hula Valley, Israel, on August 20 2007; see ambient conditions over the area in Table 1.

Thermography

The radiometric imager (FLIR SC2000), equipped with a 45° FOV lens was mounted looking straight down over an opening in the aircraft floor, and the GPS antenna was mounted under the front windshield. Given the 0.20 s GPS acquisition interval at 40 m s⁻¹ ground speed, location accuracy in the flight direction was ±8 m. Image acquisition was recorded at 2 frames s⁻¹ with 0.01 s accuracy. Flights were directed along the rows by visible wheel paths of the lateral irrigation system in the sprinkler fields, and by flag bearers on the ground in the drip irrigated fields. The flight altitude was 45–50 m above ground, adhering to Israeli ceilings for agricultural aerial applications, which resulted in swath widths of 45–50 m. The ground pixel sizes obtained were about 0.15 m across the flight direction, but due to ‘smear’ caused by the slow shutter speed pixel size increased to 0.3 m along the path.

Table 1 Survey dates, times (GMT + 2), field cover and ambient conditions

Date	Swath width/density (m)	Field cover (%)	Start time (h)	End time (h)	Air temp. (°C)	Relative humidity (%)	Wind (m sec ⁻¹)	Radiation (W m ⁻²)
<i>Ground survey</i>								
18 June	1.5/24	4	12:32	13:55	32.4	37.6	4.2	955
2 July	4.5/24	19	13:20	14:29	31.0	44.6	3.4	873
8 July	4.5/12	38	12:37	14:41	32.5	42.4	3.5	850
23 July	4.5/12	38	12:29	13:38	32.3	47.0	3.2	908
2 August	4.5/12	38	12:23	13:45	33.4	41.1	2.6	926
29 August	4.5/12	38	12:52	13:51	35.4	31.9	3.2	840
<i>Aerial survey</i>								
20 August	45–50	80–120%	12:18	13:15	34.0	34.8	2.3	920

Image processing and map generation

Original images of 45×33 m in size were subdivided during processing into six equal sub-frames of two rows and three columns covering a crop area of about 250 m^2 . The CWSI was evaluated for each sub-frame as described by Eqs. 1–3. The center location of each sub-frame was calculated from the frame's GPS center point, elevation and azimuth data using basic trigonometry (Fig. 4). Each CWSI value was assigned to the center point of the sub-frame. Maps of water stress were generated in ArcView by IDW interpolation as described in the ground surveys.

Results and discussion

Ground measurements

Site selection validation

The first survey was done 1 day before the commencement of irrigation. An overview of the test area showing LWP sampling point locations overlaid on the June 18 CWSI map is shown in Fig. 5a. The extents of stress levels at the ten sampling points are illustrated in Fig. 6 where crop height, crop cover and LWP are closely correlated. Main stem elongation rates and LWP are established crop stress indicators in cotton (Grimes and Yamada 1982; Howell and Meron 2007). In the absence of watering before the first irrigation, the cotton consumed the water stored in the soil, and water stress developed as a function of the different water holding capacities of the soil in various sections of the field (Fig. 5). Plants growing in more sandy soil with low water holding capacity consumed all the available water, and remained small and deeply stressed. Conversely, plants growing in soil with higher water capacity flourished.

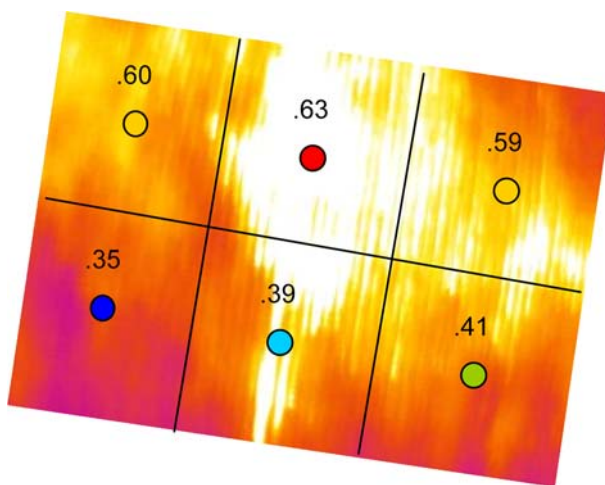


Fig. 4 Ground referenced thermal image showing image division and the points of CWSI assignments

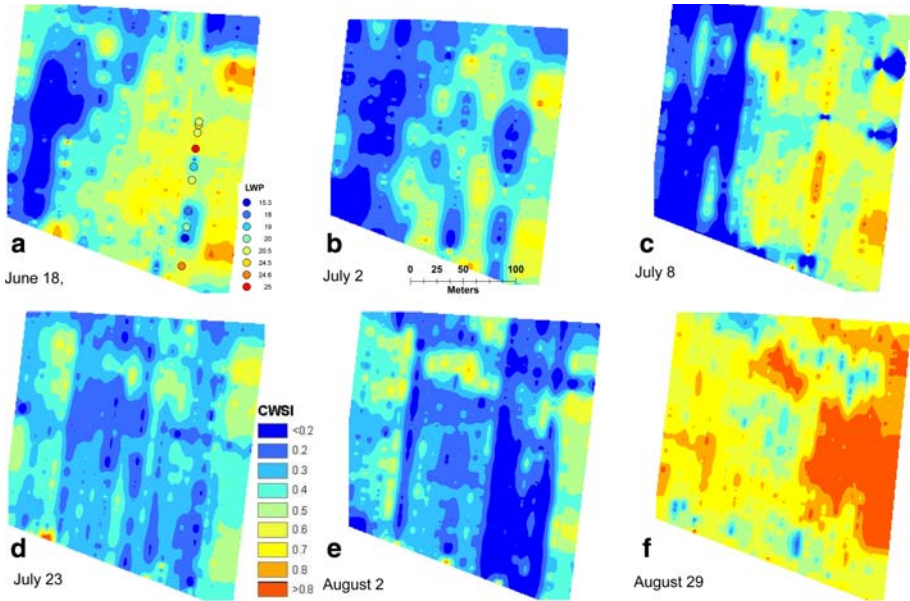
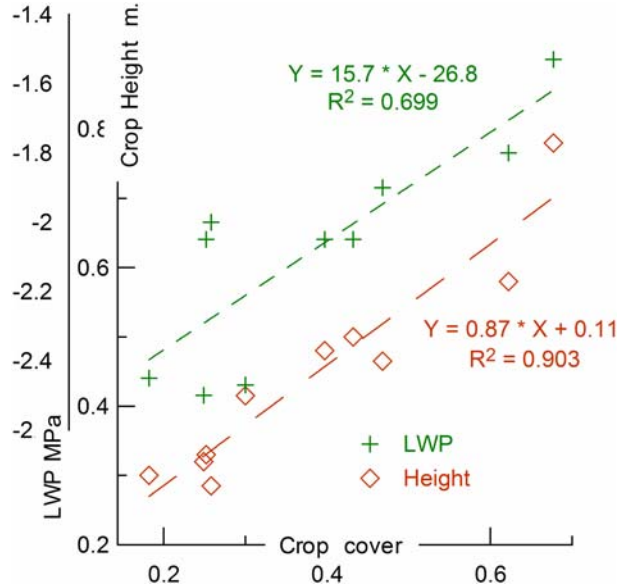


Fig. 5 Cotton CWSI maps of the field monitored in the Hula Valley acquired on six separate days by ground survey in 2007. The LWP sampling points for 18 June are shown in map a. Distance scale in 5 b

Fig. 6 Relationships between crop cover, crop height and LWP on 18 June 2007, before the first irrigation in the monitored field



Crop stress monitoring during the season

The maps in Fig. 5 show the results from six ground surveys. Stress levels on the survey dates are the outcomes of irrigation timing and the amounts of water applied (Fig. 1).

The second survey (Fig. 5b) was done after the second irrigation, and the third survey (Fig. 5c) was immediately before the third irrigation was applied. The soil water deficit is evident from the ETp and water applied during the first two irrigations (Fig. 1, arrows 1 and 2). Corresponding plant stress levels in Fig. 5b and c show the deficit clearly, mainly in the soil with low water holding capacity.

The amount of water applied was increased at the third irrigation to reach 100% ETp (Fig. 1, arrows 3–5). The fourth survey (Fig. 5d), immediately before the fourth irrigation, shows the moderate stress levels that were expected. In the fifth survey (Fig. 5e), before the fifth irrigation, the plants on the more sandy soil appear to be less stressed than those on soil with a higher water holding capacity. This contradiction can be explained, by the fact that plants grown in soil with a low water holding capacity were smaller, with reduced crop cover and less surface exposed to transpiration. Their estimated water consumption was closer to 70% ETp, therefore, with the amount of water applied to replace full ETp they were over irrigated. The last ground survey (Fig. 5f) was done after considerable stress was developed by reducing irrigation before defoliation. The stress is evident in the entire field, and it became more enhanced in the rapidly drying sandy soil.

Relation of CWSI to leaf water potential

Leaf water potentials (Fig. 7) correlated linearly ($R^2 = 0.816$) with CWSI over the full range of crop stress recorded during the season. The scatter is considerable in the part of the graph representing the well-watered range, from the origin to a CWSI of 0.4 (~ -1 to -1.5 MPa LWP). This scatter makes it difficult to fine-tune stress detection within this range. However, the stressed range above CWSI 0.4 is clearly discernible from the well-watered range. According to this result, CWSI can replace LWP for cotton water-stress evaluation, at least as an indicator of stress or no-stress. The importance of this finding is that it enables aerial thermography, which is a fast and efficient tool for monitoring and mapping crop stress over wide areas, to be used for managing irrigation

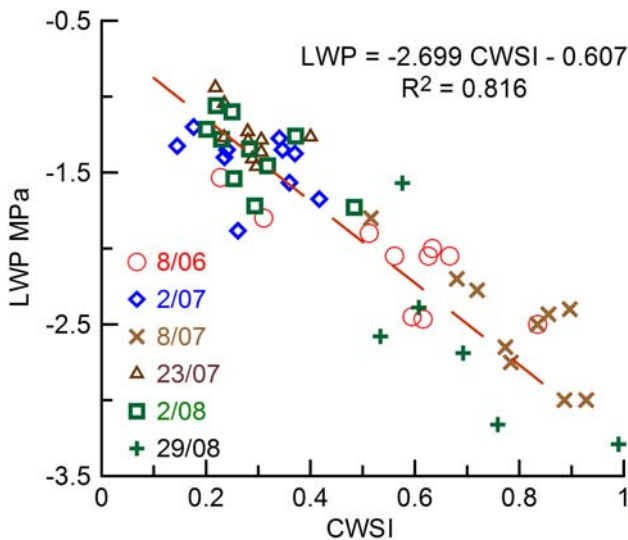


Fig. 7 Relation of cotton CWSI to leaf water potentials in six scanning days, at the monitored field in the Hula Valley 2007

Aerial survey

The aerial surveys of August 20, 2007 included two lateral moves, one center pivot and one drip irrigated field. The peanut field (Fig. 8) was scanned while irrigation water was being applied; the lateral move position is indicated by the arrow. Mean CWSI levels and CWSI histograms, calculated from the interpolated values on the mapping grid, are shown on the figure. Stress levels are 0.2 CWSI units less after irrigation, and are less scattered on the histogram. In the drip-irrigated process tomato field (Fig. 9) stress levels are quite moderate, but less uniform than expected from such an even water distribution system. Factors other than water distribution uniformity appear to have contributed to the variation in crop stress in this field.

The cotton field where the ground monitoring took place was scanned by the aerial survey 1 day before the final irrigation, and the stress map is shown in Fig. 10. The western part of the field, where the irrigation cycle begins, is more stressed with CWSI values about 0.2 units higher than in the eastern part. Variation in stress levels evident in the field is the result of incremental outcomes of previous irrigations and soil water holding capacities; they are increasingly discernible with time after the previous irrigation. The polygon

Fig. 8 Water stress map of a peanut field during irrigation on 20 August 2007. Mean CWSI values are indicated ahead and behind the lateral move position (arrow)

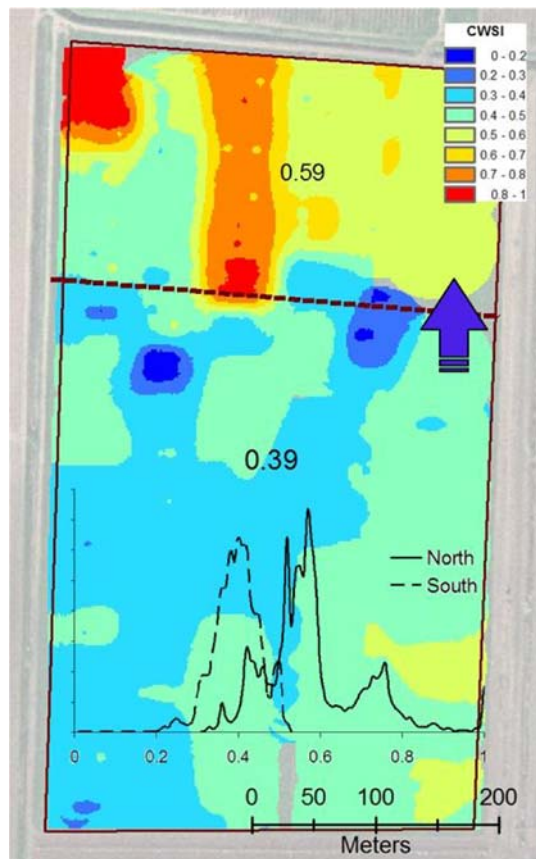
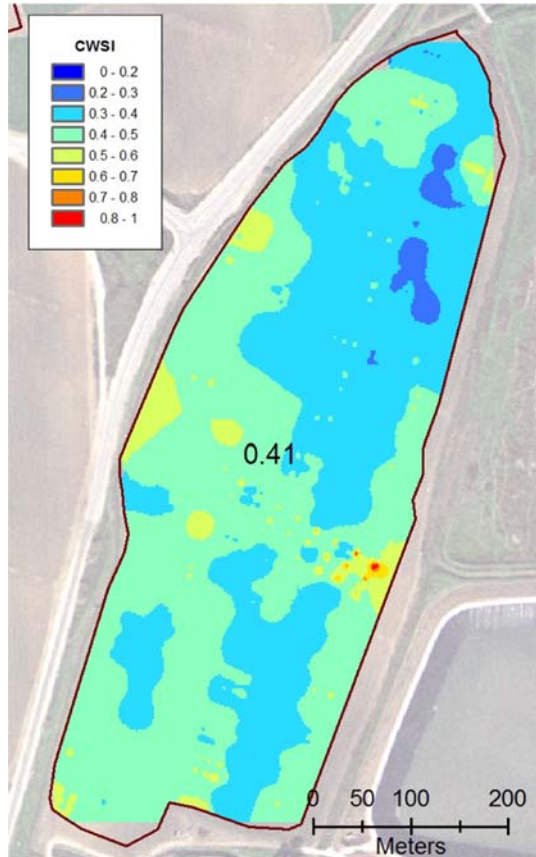


Fig. 9 Water stress map of a drip irrigated process tomato field on 20 August 2007



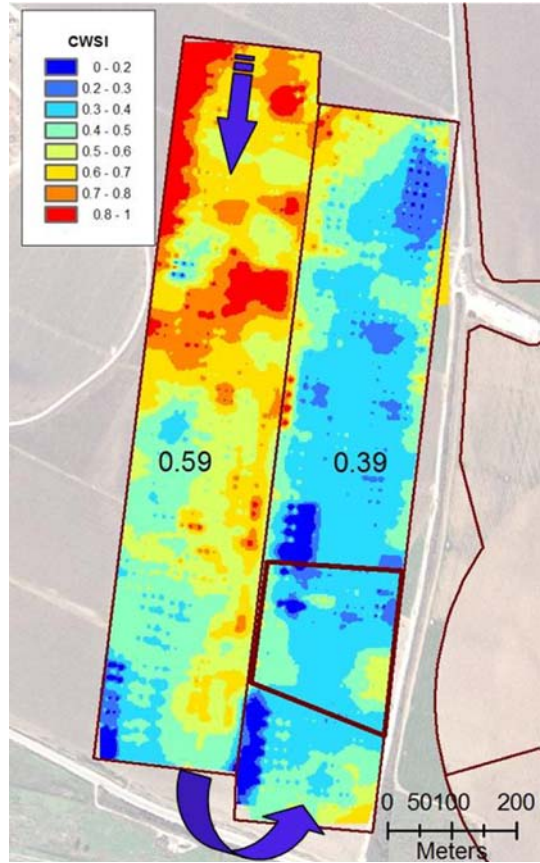
marked on the stress map in Fig 10 is less detailed compared to the ground stress maps of the same section (Fig. 5f) as the resolution of the aerial scan was much coarser than that of the ground scan. After the final irrigation in the center-pivot cotton field (Fig. 11), overall stress levels were high, but a difference of 0.14 CWSI units is still discernible between the earlier and more recent irrigation dates.

Applications in irrigation management

Moving irrigation machines

Irrigation machines based on a center pivot or that move laterally can be sub-sectioned, and the sections can then be controlled separately with technology that already exists and with relatively little additional investment. The potential for variable-rate, site-specific water application is shown by Fig. 12, which was surveyed from the ground on June 18 (Fig. 5a) before the first irrigation. Once such maps are available there are several choices; for example, pre-irrigation of the stressed sections only or application of different amounts of water according to the stress levels. Other related spatial information derived from the

Fig. 10 Water stress map of a cotton field before last irrigation on 20 August 2007. *Arrows* indicate lateral move position and pivoting directions of the irrigation rig. Numbers are the mean CWSI levels for the East and West parts of the field. The bold polygon marks the ground monitored part of the field



same scan, such as crop cover and plant height, or other sources such as yield maps or soil information, could refine site-specific irrigation management further.

Solid set irrigation

Maps provide valuable visual information, but they need additional processing to quantify the information for management. Digital map information on crop stress enables spatial statistics to be computed from the CWSI data on a grid, and numeric reporting of crop stress levels for each management zone (Fig. 13). The grower can assess mean values of crop water status, the distribution of stress levels around the mean and the extent of water stress extremes in the field at a glance on the graph, without studying the maps. This is particularly important in solid set systems where irrigation is managed in whole units controlled by a single valve. When crop water stress is monitored routinely, short-term changes in stress levels from previous scans can be related directly to changes made in the management of irrigation. The CWSI mean and dispersal statistics also enable the scheduling of irrigation to suit drier, wetter or average stress levels. In the long term, stress maps enable reorganization of irrigation zones according to uniformity criteria.

Fig. 11 Water stress map of a center pivot irrigated cotton field after the last irrigation on 20 August 2007. *Scattered line and arrow* indicate final pivot position and turning directions of the irrigation rig

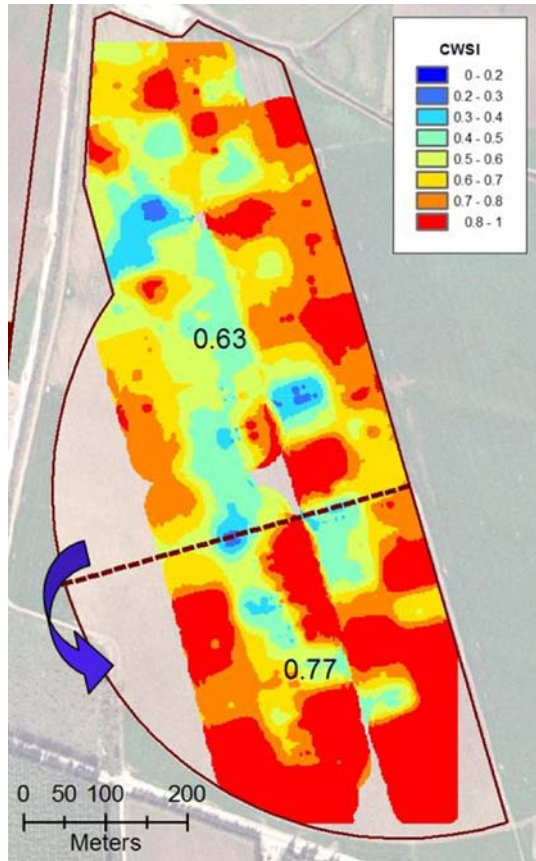
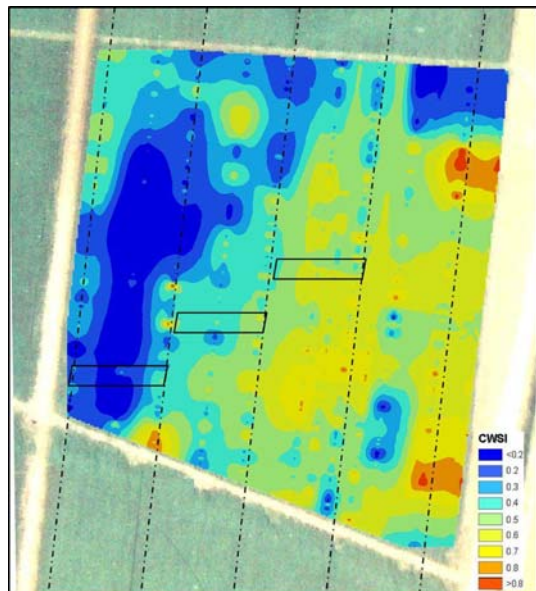


Fig. 12 Management zones in a per-section controlled variable-rate lateral move irrigator. *Scattered lines* are wheel paths



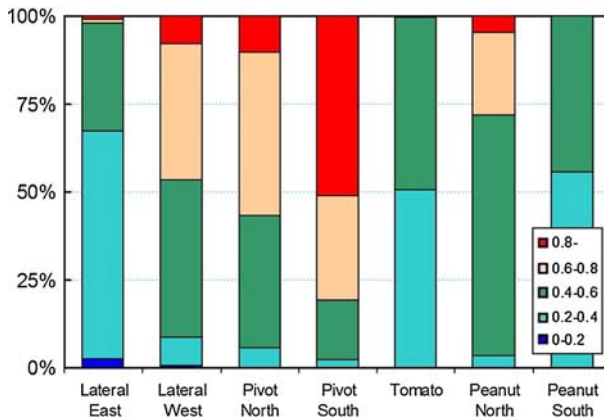


Fig. 13 Mean crop stress levels (CWSI) and their distribution for the August 20 aerial survey fields shown in Figs. 8, 9, 10, 11

Conclusions

A set of thermal remote sensing surveys were conducted from ground and low flying aerial platforms in the Hula Valley of Israel to provide crop stress maps, a prerequisite of site-specific irrigation management.

Leaf water potentials of cotton measured at 10 fixed sampling points during the season related linearly ($R^2 = 0.816$, $n = 56$) to CWSI at the same position, processed by the reported procedure. The range of values indicating stress was clearly separated from the well-watered range. This finding opens the door to simplification of thermal image evaluation by histogram analysis, eliminating the need for much more complex visible image co-registration and sunlit foliage pattern recognition processing.

The CWSI maps generated from the ground surveys of the cotton field corresponded well to irrigation history and to the calculated soil water balance. Spatial variability in the aerial stress maps of peanuts, process tomato and cotton fields could have been related to distinct irrigation events on the ground. These results suggest that this method could be extended to other crops after crop specific calibration of the imagery.

According to the methods tested and developed, aerial thermography can provide the maps needed for site-specific irrigation management. Post processing of the maps to indicate particular levels of stress in irrigation machine sections of the field can provide a template for the machine to deliver spatially variable rates of irrigation. Beyond direct visual evaluation, stress statistics in management zones derived from the map database, enables the grower to make quantitative scheduling decisions for both mobile or static irrigation.

Acknowledgments This research was supported by Grant No TB-8006-04 from BARD, the US – Israel Binational Agriculture Research and Development Fund. Support to this research was provided by the Min. of Agriculture Chief Scientist Office Grant No. 458-0361-05. Aerial survey was made possible by a contribution of Chim-Nir Israel (www.cnairways.com). The authors appreciate the cooperation of “Gadash Shemes Cooperative”, Amir, Israel, in the field operations.

References

- Camp, C., Sadler, E. J., & Evans, R. G. (2006). Precision water management: Current realities, possibilities and trends. In A. Sirwansan (Ed.), *Handbook of precision agriculture* (pp. 153–183). Binghamton NY: The Haworth Press.
- Cohen, Y., Alchanatis, V., Meron, M., Saranga, Y., & Tsipris, J. (2005). Estimation of leaf water potential by thermal imagery and spatial analysis. *Journal of Experimental Botany*, *56*, 1843–1852.
- Craddock, E. (1994). The California irrigation management information system (CIMIS). In G. J. Hoffman, T. A. Howell, & K. H. Solomon (Eds.), *Management of farm irrigation systems* (pp. 931–941). St. Joseph MI: American Society of Agricultural Engineers.
- Gardner, B. R., Nielsen, D. C., & Shock, C. C. (1992a). Infrared thermometry and the crop water stress index. 1. History, theory, and baselines. *Journal of Production Agriculture*, *5*, 462–466.
- Gardner, B. R., Nielsen, D. C., & Shock, C. C. (1992b). Infrared thermometry and the crop water stress index. 2. Sampling procedures and interpretation. *Journal of Production Agriculture*, *5*, 466–475.
- Grimes, D. W., & Yamada, H. (1982). Relation of cotton growth and yield to minimum leaf water potential. *Crop Science*, *22*, 134–139.
- Howell, T. A., & Meron, M. (2007). Irrigation scheduling. In F. R. Lamm, J. E. Ayars, & F. S. Nakayama (Eds.), *Microirrigation for crop production* (pp. 61–131). Amsterdam: Elsevier.
- Idso, S. B. (1982). Non-water-stressed baselines: A key to measuring and interpreting plant water stress. *Agricultural and Forest Meteorology*, *27*, 59–70.
- Jackson, R. D., Idso, S. B., Reginato, R. J., & Pinter, P. J. (1981). Canopy temperature as a crop water stress indicator. *Water Resources Research*, *17*, 133–138.
- Jones, H. G. (1999). Use of infrared thermometry for estimation of stomatal conductance as a possible aid to irrigation scheduling. *Agricultural and Forest Meteorology*, *95*, 139–149.
- Kim, Y. J., Evans, R. G., & Iversen, W. M. (2007). The future of intelligent agriculture. Wireless site-specific irrigation. *Engineering & Technology for a Sustainable World* (electronic publication of the ASABE, St Joseph MI), *15*(1), 2–3.
- Leinonen, I., & Jones, H. G. (2004). Combining thermal and visible imagery for estimating canopy temperature and identifying plant stress. *Journal of Experimental Botany*, *55*, 1423–1431.
- Meron, M. (1987). Measurement of cotton leaf temperatures with imaging IR radiometer. In R. J. Hanks & R. W. Brown (Eds.), *Proceedings of international conference on measurement of soil and plant water status* (pp. 111–113). Logan, UT: Utah State University.
- Meron, M., Grimes, D. W., Phene, C. J., & Davis, K. R. (1987). Pressure chamber procedures for leaf water potential measurements of cotton. *Irrigation Science*, *8*, 215–222.
- Meron, M., Tsipris J., & Charitt, D. (2003). Remote mapping of crop water status to assess spatial variability of crop stress. In: J. Stafford & A. Werner (Eds.), *Proceedings of 4th European conference on precision agriculture* (pp. 405–410). Wageningen, The Netherlands: Wageningen Academic Publishers.
- Or, D. (1995). Soil water sensor placement and interpretation for drip irrigation management in heterogeneous soils. In F. R. Lamm (Ed.), *Proceedings of fifth international microirrigation conference* (pp. 214–221). St Joseph, MI: ASABE.
- Peters, R. T., & Evett, S. R. (2004). Complete center pivot automation using the temperature-time threshold method of irrigation scheduling, (Paper No 042196, pp. 1–12). ASAE/CSAE Annual International Meeting, Ottawa, Ontario, Canada.
- Schmitz, M., & Kuyper, M. C. (1998). Soil moisture sensors in field application, a comparative study. *Zeitschrift für Bewässerungswissenschaft*, *33*, 87–102.
- Schmitz, M., & Sourell, H. (2000). Variability in soil moisture measurements. *Irrigation Science*, *19*, 147–151.